OPEN ACCESS

UNIVERSITY OF DUNDEE

University of Dundee

Determining paediatric patient thickness from a single digital radiograph – a proof of principle

Worrall, Mark; Vinnicombe, Sarah; Sutton, David G.

Full title: Determining paediatric patient thickness from a single digital radiograph – a proof of principle

Shortened title: Paediatric patient thickness from a digital radiograph

Manuscript type: Full paper

Mark Worrall[1] MSc, Sarah Vinnicombe[2] BSc MRCP FRCR, David G Sutton[1] PhD

[1]Medical Physics, Ninewells Hospital and Medical School, Ninewells Avenue, Dundee, DD1 9SY, UK

[2]Division of Imaging and Technology, Ninewells Hospital and Medical School, University of Dundee, Dundee, DD1 9SY, UK

Abstract

Objectives: This work presents a proof of principle for a method of estimating the thickness of an attenuator from a single radiograph using the image, the exposure factors with which it was acquired and a priori knowledge of the characteristics of the x-ray unit and detector used for the exposure. It is intended this could be developed into a clinical tool to assist with paediatric patient dose audit, for which a measurement of patient size is required.

Methods: The proof of principle used measured pixel value and effective linear attenuation coefficient to estimate the thickness of a Solid Water attenuator. The kerma at the detector was estimated using a measurement of pixel value on the image and measured detector calibrations. The initial kerma was estimated using a look up table of measured output values. The effective linear attenuation coefficient was measured for Solid Water at varying kV_p. Eleven test images of known and varying thicknesses of Solid Water were acquired at 60, 70 and $81kV_p$. Estimates of attenuator thickness were made using the model and the results compared to the known thickness.

Results: Estimates of attenuator thickness made using the model differed from the known thickness by 3.8mm (3.2%) on average, with a range of 0.5 – 10.8mm (0.5 – 9%).

Conclusions: A proof of principle is presented for a method of estimating the thickness of an attenuator using a single radiograph of the attenuator. The method has been shown to be accurate using a Solid Water attenuator, with a maximum difference between estimated and known attenuator thickness of 10.8mm (9%). The method shows promise as a clinical tool for estimating abdominal paediatric patient thickness for paediatric patient dose audit, and is only contingent on the type of data routinely collected by Medical Physics departments.

Advances in knowledge: A computational model has been created that is capable of accurately estimating the thickness of a uniform attenuator using only the radiographic image, the exposure factors with which it was acquired and a priori knowledge of the characteristics of the x-ray unit and detector used for the exposure.

1. Introduction

The methodology proposed for paediatric patient dose audit for radiographic examinations in the UK[1] relies upon either a physical measurement of the thickness of the patient in the examination orientation or an equivalent cylindrical diameter (ECD) derived from the patient's height and weight so that the examination Kerma Area Product (KAP) or Entrance Surface Dose (ESD) can be corrected to that of the nearest standard sized patient. The correction involves taking the ratio of the patient thickness to the defined thickness of the closest sized standard paediatric phantom and using this ratio to correct the patient's examination KAP to a normalised KAP value akin to that which would have been received by the standard paediatric phantom if it had undergone the examination. This approach has seen international endorsement[2].

All national patient dose audits undertaken in the UK since this method was proposed[3-5] have had insufficient paediatric data provided with patient thickness or ECD to allow this preferred methodology to be used; this despite a specific effort to directly target 16 children's hospitals in 2010[5]. The authors were forced to conclude that it was not practical to make thickness or height and weight measurements of the patient at the time of the examination and no updated paediatric reference doses were proposed for radiographic examinations[5].

Since the adoption of the first National Diagnostic Reference Levels (NDRL) for paediatric examinations in the UK in 2000 there have been significant changes to equipment; there has been a step change to Computed Radiography (CR) and Direct Digital Radiography (DDR). Paediatric examinations undertaken using these technologies have no relevant national comparator, preventing an important part of the optimisation cycle[6].

Given the higher risk from ionising radiation to paediatric patients due to their increased radiosensitivity and longer life expectancy[7], it is important that some means of overcoming the problems with paediatric dose audit be devised.

If the process of patient thickness estimation were to be somehow automated, this would remove this significant barrier to paediatric patient dose audit and allow for the vital comparative dosimetry information necessary for examination optimisation. It is proposed that a computational model be created to estimate the thickness of a patient from an unprocessed digital radiograph. The model will use reasonable assumptions following extensive simulation and verification about the clinical site under examination, the geometry of the radiograph, the imaging equipment used and the exposure factors. With this estimated thickness, the methodology proposed by the then National Radiological Protection Board (NRPB) for paediatric patient dose audit[1] can be used.

Whereas the accurate estimation of patient thickness from a single radiographic image using only information extracted from a DDR x-ray unit is the ultimate goal of this work, this paper presents the proof of principle. The proof of principle has involved developing a computational model to estimate the thickness of an attenuator of uniform composition from a single digital radiographic image and information that could be extracted from a DDR x-ray unit. As the method relies on single photon techniques, the initial clinical application will be for abdomen x-rays, since for any path through the abdomen that avoids the spine, all of the tissues exhibit roughly similar linear attenuation coefficients.

2. Theoretical overview

It is the intention to use the average Pixel Value (PV) from a region of interest (ROI) in conjunction with the exposure factors to produce an estimate of the thickness of the subject of the x-ray. All this information can be extracted from a DDR x-ray unit for any exposure undertaken.

The detector kerma, k_d, of a point source monoenergetic x-ray beam in a narrow beam geometry can be calculated using the Beer-Lambert law; $k_d = k_0 e^{-\mu x}$; $x = - \left[\dfrac{Ln\left(\frac{k_d}{k_0}\right)}{\mu} \right]$. Equation 1.

where;

- k_0 is the unattenuated kerma of the x-ray beam at the detector
- μ is the linear attenuation coefficient of the attenuating medium
- x is the distance the x-ray beam travels through the attenuating medium

As is well known, the Beer-Lambert law is not strictly applicable to clinical exposures, which employ a broad, polyenergetic x-ray beam directed through a patient composed of many different elements. However, this work will use it as an approximation. The method implicitly assumes a single phase model, and as such can only be applied in areas where there is no bony tissue.

Considering each of these variables;

a) Detector kerma, k_d

For an unprocessed radiograph, PVs are assigned in relation to the signal received across the detector according to the manufacturer's calibration. The average PV can be calculated for any sized ROI and at any location within the image. For a uniform attenuator, the ROI size is not an important consideration, but this will need consideration for clinical application. Since the practical work in this paper was undertaken using a Fuji CR system, we consider the PV calibration for Fuji, which has the form $PV = a_{kV_p,HVL} Ln(k_d\ (\mu Gy)) + b_{kV_p,HVL}$, where $a_{kV_p,HVL}$ and $b_{kV_p,HVL}$ are coefficients that are dependent upon the kV_p and Half Value Layer (HVL) of the x-ray beam incident upon the CR cassette.

As the Fuji CR cassette has an energy dependence[8], any change to the calibration conditions – an alteration to the kV_p or the addition of any attenuating material, like a patient or test object - means that the manufacturer's stated relationship no longer holds, although the form of the relationship will still be correct. Therefore, for PV calibrations undertaken using x-ray beams of varying kV_p and beam quality (characterised by its HVL), $a_{kV_p,HVL}$ and $b_{kV_p,HVL}$ are observed to change.

If the PV calibration is measured over a variety of beam qualities – achieved by making changes to kV_p and attenuation material and thickness – these relationships can be used to calculate k_d (in μGy) for any given exposure in which the attenuator and thickness is known thus;

$$k_d(\mu Gy) = e^{\left(\frac{PV - b_{kV_p,HVL}}{a_{kV_p,HVL}}\right)}.$$

Using the measured calibrations for PV at various kV_p and HVLs, it is possible to use a PV measured from the examination image to calculate a finite number of values for k_d that correspond to a range of values of HVL at the known examination kV_p. One of these will be the correct value of k_d, but since the thickness of the attenuator is unknown, the HVL is also unknown and so the correct value of k_d cannot be identified.

Whilst a calibration for PV with detector signal can be measured for any processing applied – such as that used to present the image clinically – these calibrations are different for all available clinical processing algorithms. The advantages of using unprocessed radiographs are that only a single cohort of calibrations need to be performed and these will not be subject to change at any point in the detector lifetime.

b) Unattenuated kerma, k_0

k_0 can be estimated using the examination kV_p, mAs, Focus to Detector Distance (FDD) and field size. For an x-ray machine, the output in terms of μGy/mAs at 100cm FDD for varying kV_p at the centre of the x-ray field is a commonly undertaken measurement for the purposes of Quality Assurance (QA).

There is a dependence of the measured μGy/mAs on field size; the measured value at the centre of a 40 x 40cm field was 10% higher than at the centre of a 10 x 10cm field at 81kV_p for an equivalent mAs. Therefore the value must be measured for varying field sizes. If values of μGy/mAs at 100cm FDD varying with field size and kV_p are made available in a look up table, the appropriate value can be corrected for examination mAs and FDD to give an estimate of k_0.

c) Effective linear attenuation coefficient, $μ_e$

A linear attenuation coefficient is a number that relates to the probability of an x-ray being attenuated by a material. The linear attenuation coefficient is unique to a single energy and a single material. In this instance, the x-ray beam is composed of multiple x-ray energies, characterised by a kV_p and with a defined HVL.

As there are multiple x-ray energies, an effective linear attenuation coefficient can be used[1]. This can be defined as; $μ_e = Ln \left(\frac{Exit\ kerma}{Entrance\ kerma} \right)$. This is a value that can be calculated using measured values of exit and entrance kerma for any material using any x-ray beam. Note that the value of $μ_e$ that is calculated will be specific to that x-ray beam (characterised by kV_p and HVL) and the material composition and thickness. It is well known that $μ_e$ calculated using measurements made through 1mm of a material will not be the same as the $μ_e$ calculated using measurements made through 10mm of the same material normalised to a 1mm thickness (i.e. divided by 10) because in the latter case beam hardening will affect the x-ray beam to a greater extent as it passes through the material, increasing its HVL and reducing the value of $μ_e$.

For any clinical projection, the types of tissues the x-ray beam will pass through are known, as is the range of composition for each tissue when patient variation is accounted for. Hence $μ_e$ can be measured using materials designed to mimic those tissues or simulated using Monte Carlo techniques. In both cases, $μ_e$ can be derived for multiple x-ray beams, characterised by their kV_p and HVL.

Multiple μ_e can be measured or simulated for varying tissue thicknesses for varying combinations of kV_p and pre-attenuation HVLs. These can be applied as appropriate during the calculation in Equation 1.

d) Calculation of object thickness

Once k_d, k_0 and μ_e have been determined, the attenuator thickness can, in principle, be calculated using equation 1. From the discussion so far in section 2, it can be seen that

i) There will have been many values calculated for k_d from the PV calibrations that have been measured. The most accurate of these cannot be predicted theoretically because the HVL of the x-ray beam exiting the material is unknown.

ii) It is possible to select a single value of k_0, using data from a look up table of values ordered by kV_p and field size and corrected for examination mAs and FDD.

iii) There will be many values available for μ_e; the examination kV_p is known but the value of μ_e is dependent upon the unknown attenuator thickness.

The experimental steps taken to explore the three factors outlined above are outlined in section 3.

3 Methods and results

3.1 Materials

For the experimental work, all exposures were made using a Philips Optimus 50 radiographic x-ray system. The x-ray system was up to date in terms of servicing and QA and was known to be performing to specification throughout. The system was warmed up with a minimum of 10 exposures prior to any use.

Although it is proposed that this approach be used for DDR, this work was performed using a Fuji CR system for reasons of greater local access for the necessary measurements. As preliminary work indicated significant variation in the measured average PV between CR cassettes for equivalent exposures, all images were acquired on a dedicated Fuji CR cassette, acquired for this work and never used clinically. The same Fuji XG5000 CR multi-loader was used for processing the cassette each time.

All kerma measurements were made using a Raysafe Solid State Radiographic / Fluoroscopic (R/F) detector with a calibration uncertainty of 5% traceable to a national standard.

The attenuator used throughout was Solid Water High Equivalency (HE) (Gammex), in 20 x 20cm blocks of total thickness 20cm divided such that any thickness can be achieved between 0.5 and 20cm in 0.5cm increments. Solid Water HE uses nanospheres to create homogeneous slabs that mimic true water within 0.5% at diagnostic energies[9].

HVLs were measured using 99% minimum purity aluminium available in 10x10cm sheets up to a total thickness of 10mm with any thickness between 0.1mm and 10mm in 0.1mm increments available.

3.2 Measurement of k_d

a) Variation of HVL with thickness of attenuator - methodology

As explained in section 2a, k_d was estimated using detector PV calibrations made at varying kV_p and HVLs. To determine how the HVL varies at the exit surface of an attenuator as it varies in thickness, measurements of HVL were made in a broad field geometry, in a position that is inclusive of scatter. This broad field, inclusive scatter geometry is the clinically relevant scenario and is shown in figure 1a. For comparison, measurements of HVL were also made using a narrow beam and in a position that avoids scatter as much as possible. This narrow field, reduced scatter geometry is like the conventional technique used to verify x-ray tube filtration and is shown in figure 1b.
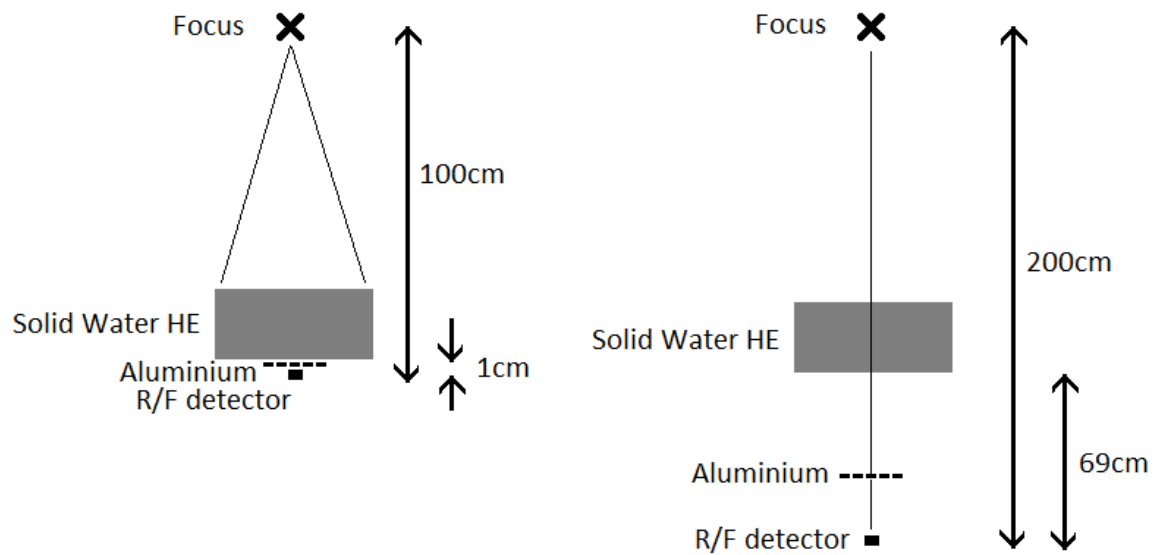

Figure 1: (a) the broad field, inclusive scatter geometry and (b) the small field, reduced scatter geometry used for measuring the HVL of the x-ray beam

For the broad field, inclusive scatter geometry, the R/F detector was placed 100cm from the x-ray tube focus in line with the central axis. Thicknesses in the range of 1 - 20cm of Solid Water HE were positioned with the exit surface 1cm above the R/F detector. The x-ray field size measured 30x30cm at the R/F detector. Exposures were made at 60, 70 and 81kV_p and 5 – 50mAs (the selected value varied for different attenuator thicknesses but was kept constant for a single thickness). Increasing thicknesses of aluminium were placed directly above the R/F detector until the measured kerma dropped to half of that measured with no aluminium present. A broad field, inclusive scatter HVL was then estimated for each of the thicknesses of Solid Water HE used from logarithmic plots of aluminium thickness vs. measured kerma.

The method was the same for the small field, reduced scatter geometry but the geometry was different; the R/F detector was placed 200cm from the x-ray tube focus in line with the central axis. The exit surface of the attenuator was 69cm above the R/F detector. The x-ray field size measured 3x3cm at the R/F detector (the smallest that could be achieved with this equipment). Increasing thicknesses of aluminium were placed in a jig 20cm above the R/F detector.

b)   *Variation of HVL with thickness of attenuator - results*

The HVLs measured for the exit beam from increasing thicknesses of Solid Water HE attenuator in broad field, inclusive scatter and small field, reduced scatter geometries at 81kV_p are shown in figure 2.
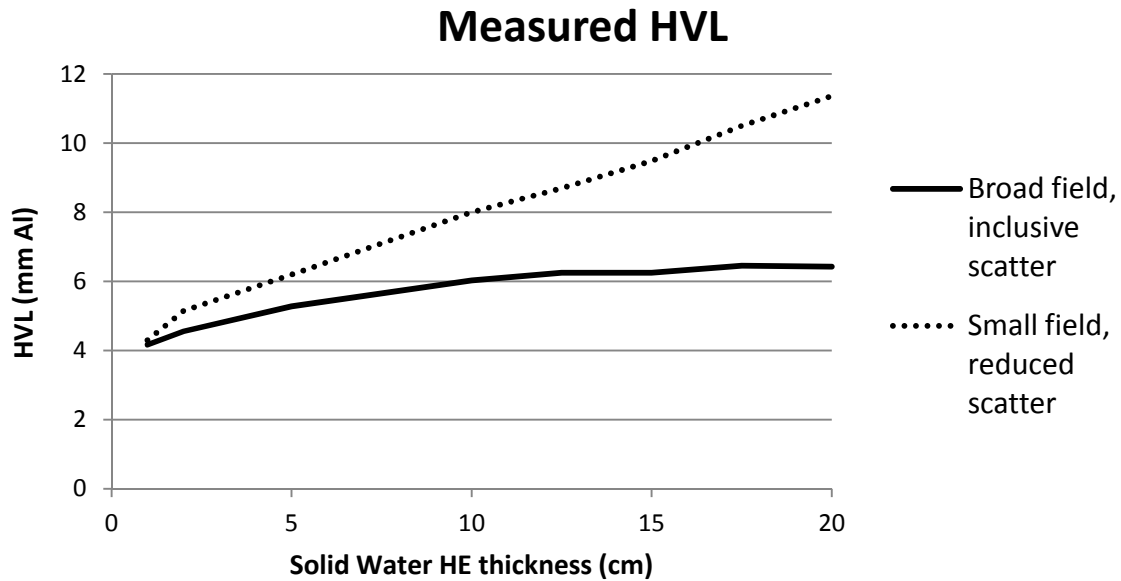
Figure 2: The broad and narrow field HVLs measured for increasing thicknesses of attenuator at $81kV_p$

As expected, the HVL for the small field, reduced scatter geometry continued to increase with increasing attenuator thickness. This is not the case for the HVL of the broad field, inclusive scatter geometry however, which increased far less quickly at about 10cm of Solid Water HE attenuator. This is because in addition to transmitted primary radiation, the detector is also measuring scattered x-rays whose average energy is significantly lower than the transmitted primary. The average HVL of the $81kV_p$ exposures made in the broad field, inclusive scatter geometry from 10 – 20cm of Solid Water HE attenuator is 6.28mm of Aluminium with a standard deviation of 0.17.

This change in HVL with increasing thicknesses of attenuator in a broad field, inclusive scatter and small field, reduced scatter geometry was also observed at 60 and $70kV_p$. Thus, a single value of HVL can be assumed for any exposure at a known kV_p and undertaken in a clinical geometry where the attenuator has an HVL in excess of that at which it begins to plateau. This will vary with x-ray unit as it is dependent upon the inherent filtration of the x-ray system and the attenuator combined, though it is likely to be near to equivalent to the case presented here – a standard diagnostic x-ray set with an attenuator equivalent to a thickness of 10cm of Solid Water HE. This should be appropriate for abdomen examinations of most paediatric patients.

c) Calibration of PV - methodology

The R/F detector was placed 150cm from the x-ray tube focus on the x-ray table at the centre of the field. Thicknesses of 1, 2, 5, 10, 12.5, 15, 17.5 and 20cm of Solid Water HE were placed just above the detector with a 1cm separation from the exit surface to the detector.

The field size at the detector was 40 x 40cm, ensuring full coverage of the R/F detector and the CR cassette. At 60, 70 and $81kV_p$, exposures were made using incremental values of mAs to deliver air kermas in the range of 1 - 18µGy; this encompasses the useful range of the CR cassette. The kerma for each combination of kV_p and mAs was measured three times using the R/F detector; the KAP

measured by the KAP meter at the tube output was recorded each time to ensure reproducibility between exposures.

These measurements were repeated for all kV_p and mAs combinations for all thicknesses of Solid Water HE.

Once the kerma measurements had been made, the process was repeated with the CR cassette in place of the R/F detector to make the PV measurements. The flat look up table 'sensitivity' was used, providing as close to unprocessed images as can be achieved on the Fuji CR system.

With these measurements, a broad field, inclusive of scatter calibration of the PV with kerma could be derived for each thickness of Solid Water HE used.

   d)   Calibration of PV - results

The measured calibrations of PV at $81kV_p$ with varying thicknesses of Solid Water HE attenuator are shown in figure 3.
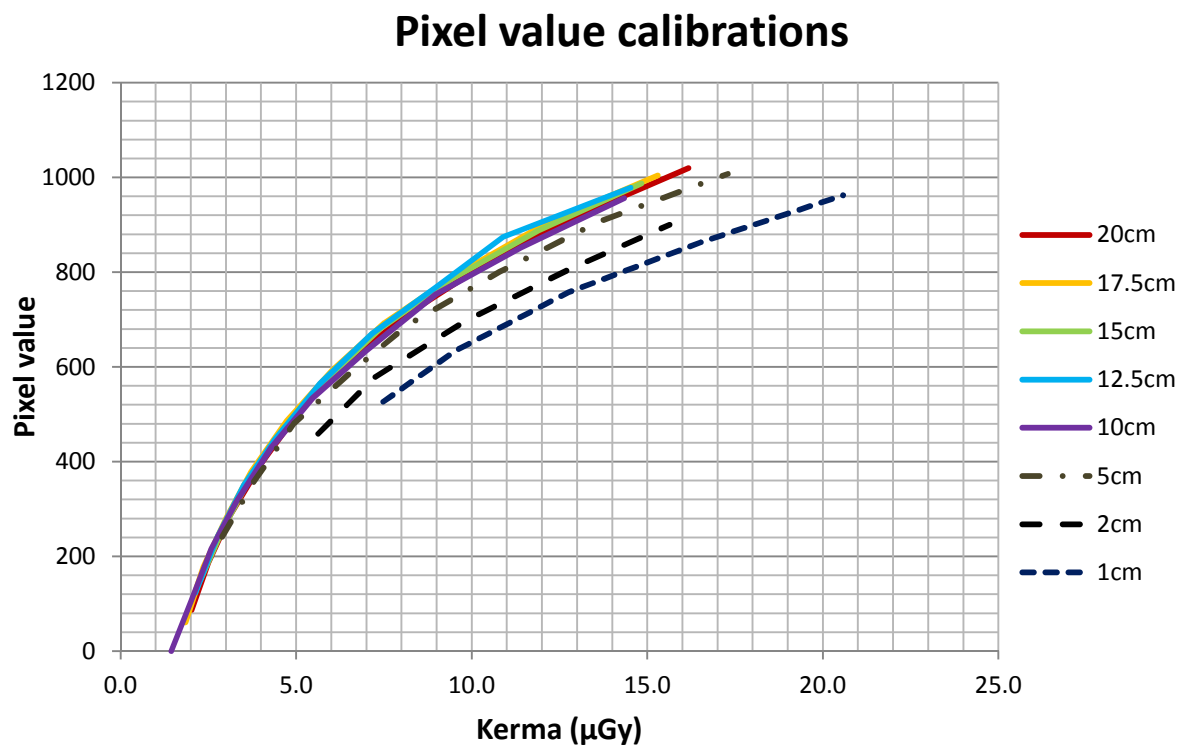
Figure 3: PV calibrations at 81kVp for varying thicknesses of Solid Water HE attenuator placed at the detector

Whilst the PV calibrations for 1, 2 and 5cm thicknesses of Solid Water HE are clearly different, the calibrations for the others are very difficult to separate. Using the 10-20cm calibrations to calculate the kerma corresponding with PV from 100 to 800 in intervals of 50 gives a maximum absolute deviation from the average of 0.37µGy, with a maximum percentage deviation of 3.76%.

This was also observed for calibrations undertaken at 60 and $70kV_p$.

Given the results of HVL in a broad field, inclusive scatter geometry already presented in section 3.2b, the variation in PV calibrations with attenuator thickness are expected. Where the broad field, inclusive scatter HVLs are different, as is the case with attenuator thicknesses in the range of 1 – 10cm of Solid Water HE, there is a distinct difference in the calibration of PV. Where the broad field, inclusive scatter HVLs become very similar, as is the case with attenuator thicknesses in the range of 10 – 20cm of Solid Water HE, the PV calibrations become difficult to distinguish.

Therefore, for a clinical examination where the patient is of sufficient size to ensure an HVL in the range where broad field, inclusive scatter HVLs plateau, a single PV calibration can be used to relate a measured PV to a kerma. Thus a value for k_d can be obtained from the PV calibrations with a minimal uncertainty.

3.3 Measurement of k_0

a) *Measurements*

Values for µGy/mAs at a 100cm FDD were measured at the centre of the x-ray beam using the R/F detector at 60, 70 and 81kV$_p$, 10mAs and a field size that varied in 5cm increments from 5 – 40cm in both the x and y axes, as shown in figure 4.
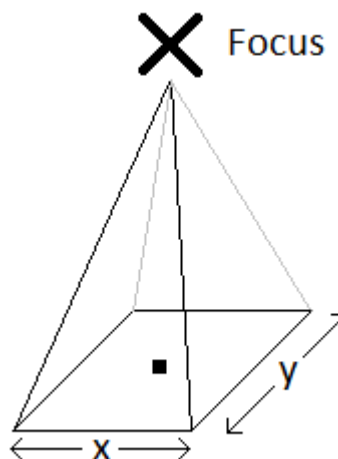
Figure 4: the x and y axes defined at the detector plane in relation to the x-ray tube focus. The R/F detector is shown in the centre of the x-ray field

Three measurements were acquired for every combination of factors and an average of the three taken to give a single value of k_0 for each combination of kV$_p$ and field size.

b) *Results*

At 81kV$_p$, values range from 45.6 to 51.1µGy/mAs; the values increased with increasing field size, as is expected due to increased scatter. At 60kV$_p$, values range from 22.8 to 25.8µGy/mAs and at 70kV$_p$ values range from 35.5 to 39.6µGy/mAs. Again, values increased with increasing field size.

3.4   Measurement of μ_e

a) Measurements

For a single material attenuator, μ_e can be found using measurements of the attenuator exit kerma and the kerma without any attenuator present via $\mu_e = -\frac{Ln\left(\frac{Attenuator\ exit\ kerma}{Attenuator\ free\ kerma}\right)}{Attenuator\ thickness}$. As the two kerma measurements are made in the same location, no correction for distance need be applied.

Measurements of attenuator exit kerma and the kerma with no attenuator present were made using the R/F detector for each of the thicknesses of Solid Water HE used for the PV calibrations at 60, 70 and 81kV$_p$. The geometry of these measurements was as for the PV calibrations.

b) Results

The variation in μ_e with increasing thickness of Solid Water HE attenuator for 60, 70 and 81kVp is shown in figure 5.
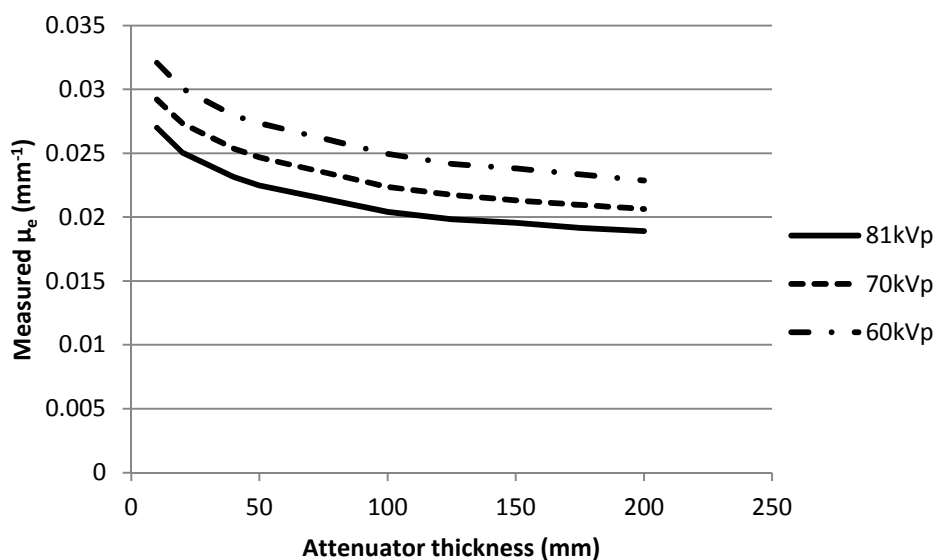
Figure 5: The variation in μ_e with increasing thicknesses of Solid Water HE attenuator

μ_e is observed to decrease logarithmically with increasing attenuator thickness, as might be expected. At an attenuator thickness of 10cm and above, the average μ_e at 60kVp is 2.39×10^{-2} mm^{-1} with a standard deviation of 8.6×10^{-4}. For the same criteria, the average and standard deviations for 70kVp and 81kVp are 2.14×10^{-2} mm^{-1} and 6.77×10^{-4}, 1.96×10^{-2} mm^{-1} and 5.86×10^{-4} respectively.

The average value of μ_e can be used for deriving the thickness of an attenuator of a clinically relevant thickness.

4   Results of model testing

The model described above was used to estimate the thickness of the attenuator for eleven images acquired at 60, 70 and 81kV$_p$ with a 100cm FDD using the dedicated CR cassette. Each image varied the thickness of Solid Water HE attenuator, the mAs and the field size.

Using a value of k$_0$ from the look up table populated using the results in section 3.3b, the value of k$_d$ derived from the average PV measured on an ROI of the image via the PV calibrations for attenuators greater than 10cm Solid Water HE presented in section 3.2d, and a value of μ$_e$ from the look up table populated from the values of attenuators greater than 10cm Solid Water HE as shown in section 3.4b, it was possible to calculate attenuator thickness from the rearranged form of equation 1.

4.1 Estimates of thickness from an unprocessed image

Two separate estimates of attenuator thickness were made; the first used the automated model, the other involved a manually calculated estimate using values for k$_d$, k$_0$ and μ$_e$ that were directly measured using the Raysafe R/F detector. These processes are summarised in the flow diagram in figure 6.

(a)

Image acquired

k$_0$ obtained from a look up table using the known examination kV$_p$, mAs and field size

Unprocessed copy made

PV of central region of interest measured

μ$_e$ obtained from a look up table using the known kV$_p$

PV converted to kerma via measured calibration (k$_d$)

Estimate x

(b)

Image acquired

k$_0$ directly measured using R/F detector

k$_d$ directly measured using R/F detector

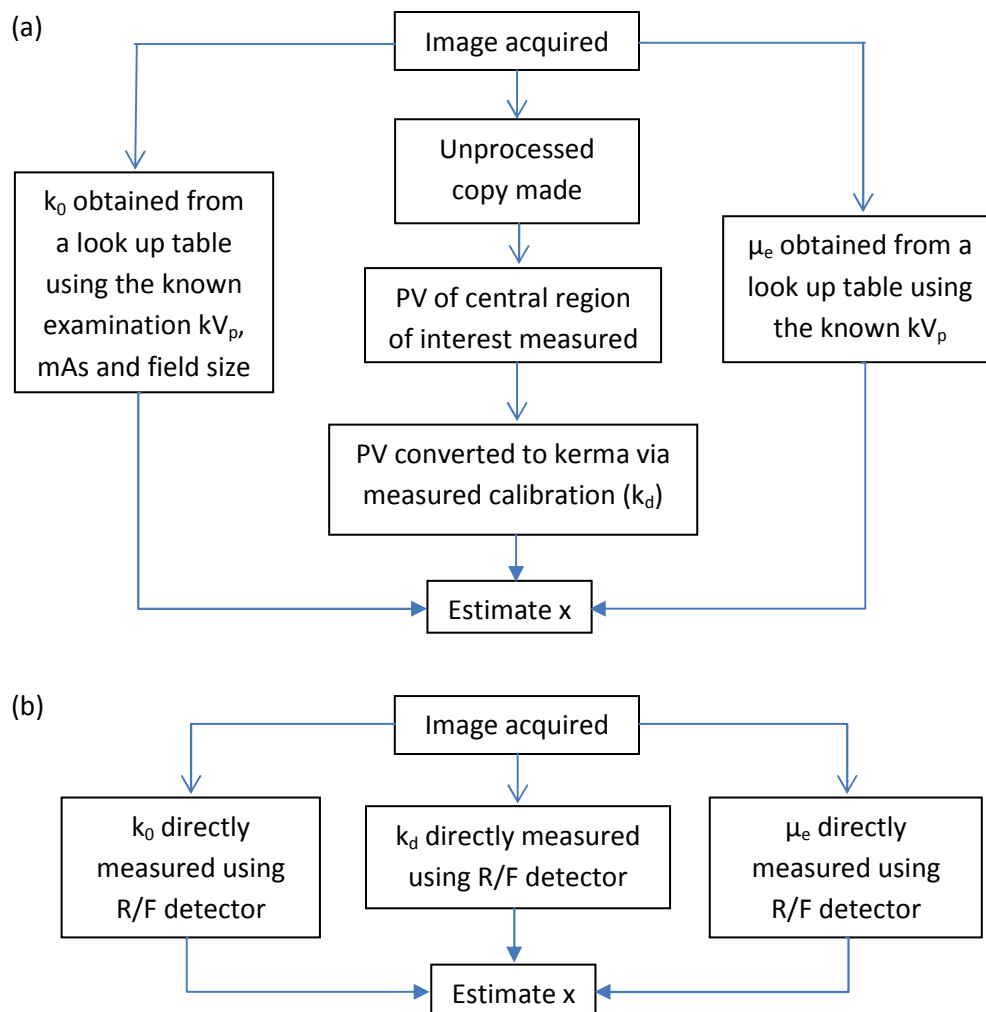μ$_e$ directly measured using R/F detector

Estimate x

Figure 6: Estimating attenuator thickness using (a) estimates of k_d, k_0 and μ_e made using the model presented in this paper and (b) direct measurements of k_d, k_0 and μ_e

The estimates of attenuator thickness made using the automated model are presented in table 1; column 4 (headed 'Automated'). The estimates of attenuator thickness that were manually calculated using the measured values of k_d, k_0, and μ_e are presented in table 1; column 5 (headed 'Manual').

Image	kV$_p$	Known attenuator thickness (mm)	Predicted thickness (mm) using;	
			Automated	Manual
1	60	110	110.7	110.0
2	60	130	131.1	132.0
3	70	115	122.4	117.4
4	70	140	144.6	142.1
5	70	170	169.5	171.5
6	81	100	109.6	102.5
7	81	120	130.8	125.2
8	81	140	143.9	143.9
9	81	165	164.3	166.8
10	81	170	180.3	181.6
11	81	190	185.0	192.6

Table 1: Predictions of attenuator thickness using the complete model and entirely measured data

The deviations in the automated model's estimation of k_d, k_0 and μ_e for each of the test images were calculated by comparing them to the measured values used for the manual calculation. These are shown in table 2.

Image	kV$_p$	Known attenuator thickness (mm)	Deviation between predicted and measured values		
			Initial kerma (k_0) (µGy)	Detector kerma (k_d) (µGy)	Effective linear attenuation coefficient (μ_e) (mm^{-1})
1	60	110	1.3 (6.0%)	0.25 (16.1%)	0.0010 (3.9%)
2	60	130	1.1 (3.0%)	0.18 (11.0%)	0.0004 (1.7%)
3	70	115	1.1 (2.5%)	0.01 (0.4%)	0.0007 (3.3%)
4	70	140	2.6 (4.9%)	0.03 (1.3%)	0.0001 (0.6%)
5	70	170	2.9 (4.2%)	0.01 (0.6%)	0.0005 (2.2%)
6	81	100	1.0 (2.1%)	0.05 (1.0%)	0.0011 (5.1%)
7	81	120	2.3 (6.3%)	0.06 (2.0%)	0.0006 (2.8%)
8	81	140	0.8 (2.7%)	0.01 (0.8%)	0.0001 (0.7%)
9	81	165	1.2 (2.1%)	0.04 (1.7%)	0.0003 (1.7%)
10	81	170	6.2 (6.6%)	0.05 (1.7%)	0.0004 (2.1%)
11	81	190	1.1 (0.9%)	0.07 (2.1%)	0.0007 (3.7%)

Table 2: The absolute and percentage differences between the values predicted by the model and the measured values for k_0, k_d, and μ_e.

The estimates made using the automated model have an absolute deviation from the known thickness that ranges from 0.5 – 10.8mm (0.5 – 9%), with an average of 3.8mm (3.2%).

The estimates made using the manual calculation resulted in a deviation from the known thickness that ranges from 0.02 – 11.6mm with an average of 3.2mm (2.2%).

Table 2 shows that the absolute error in the model's predicted values of k_d was consistently very low, ranging from 0.01 – 0.25μGy with an average deviation of 0.07μGy.

Table 2 also shows that the greatest average uncertainty in the model was associated with the estimation of k_0 from look up tables. The deviation between estimated and measured values ranges from 0.8 – 6.2μGy with an average of 1.96μGy.

The accuracy of the estimation of μ_e ranges from 0.0001 – 0.0011mm^{-1} with an average deviation of 0.0005mm^{-1}. There is a general trend in μ_e accuracy with attenuator thickness in that the deviation between estimated and measured values tends to be lower with increasing attenuator thickness. The highest values are for attenuator thicknesses close to 100mm, which is expected given the results in figure 5 showing that the rate of change in μ_e at 100mm is greater than at higher thicknesses.

5   Discussion

A computational model for estimating attenuator thickness is possible because the quality of an x-ray beam as it exits an attenuator is similar at any single kV_p in the diagnostic range, provided the attenuator thickness is in excess of 10cm of Solid Water HE or equivalent. This means a single detector kerma – PV calibration can be used to estimate the detector kerma for exposures at any given kV_p. This calibration is not dissimilar to the type routinely made by physics departments during routine QA. Estimates of initial air kerma can be made from look up tables of measured data. Estimates of effective linear attenuation coefficients can be made from measured data or Monte Carlo simulations.

Estimates of thickness for eleven test images were made using the automated model and a manual calculation from measurements made during image acquisition. As the manual estimation uses values that were directly measured for each test image, it is expected that this would give the most accurate estimate of attenuator thickness and this should be regarded as the greatest level of accuracy that can be achieved. The results of the automated estimate compare well with this standard.

Even the manually calculated method that used measured values for determining attenuator thickness does occasionally give a result with a lower accuracy (the 11.6mm absolute deviation from the known thickness for image 10 is an outlier). The fact that the estimate made using the automated model was similarly inaccurate is very suggestive of an issue with the estimation and measurement of k_0. It is likely that the initial kerma of the exposure used to generate the image deviated more from what was expected and previously measured than is usual, as radiographic x-ray units are occasionally prone to do.

It is likely to be significant that the two highest values of uncertainty are associated with the 60kV$_p$ images, indicating that there is a kV_p dependence on the accuracy of using a single calibration of PV for estimating attenuator thicknesses greater than 10cm.

There does not appear to be any trend between degree of inaccuracy and examination kV_p. The presence of a significant outlier (6.2µGy) demonstrates that the model is likely to be affected by the occasional higher than expected variation in x-ray tube output from exposure to exposure.

In considering whether this proof of principle has achieved results sufficient to merit continuation of the work, the maximum inaccuracy that can be tolerated by the end user should be considered. The aim of this work is to derive the thickness of a paediatric patient in the examination orientation and near the central axis of the x-ray beam. The current methods for obtaining this measurement are either a direct measurement using callipers or using a model with a measurement of the patient circumference as the input.

Whereas the measurement of a fixed object with callipers has a minimal uncertainty, when used with patients there are additional uncertainties associated with a reproducible measurement position. A single operator could vary their measurement position from patient to patient by many centimetres superior or inferior to where they would centre the x-ray beam. As the patient will not be of uniform thickness, this adds to the inaccuracy of the thickness measurement. In addition, abdominal breathing is normal for paediatric patients, therefore a measurement of abdominal thickness will vary throughout the breathing cycle. Accurate quantification of the uncertainty would be very patient dependent, however a 10mm deviation would not seem unreasonable.

Regarding the use of a model using a measurement of circumference as its input, there are two significant sources of uncertainty. Just as the operator may vary the position of their calliper measurement, they may also vary the position of their measurement of circumference. A variation of centimetres superior or inferior to where they would centre the x-ray beam will have more of an effect on the measurement of circumference than it would on a single dimension measurement with a calliper. As for the formulas used to estimate patient diameter from a measured circumference, those given by Hart et al[1] were derived using measurements made of European children by Bohmann[10] with the work of Lindskoug[11]. The children from which these formulas were derived were found to be 4% taller and 7% heavier than the average of a similar sample in the UK[1]. The application of these formulas to any individual patient will have a reasonable uncertainty associated with it. The thickness in the AP dimension of the abdomen of a 5 year old CIRS Atom anthropomorphic phantom (CIRS Inc., Norfolk, VA) was measured directly and compared to the estimate made using the formulas with height, weight and measured circumference as the input. Deviations of 4 – 5mm were found. For a sample of real patients, a deviation of 10mm or greater does not seem unreasonable.

Therefore the method presented in this paper does not have any greater uncertainty than that of the existing measurement options.

Just as the existing measurement options are clearly not favoured in radiology departments, does this method feature any component that would make its adoption unlikely?

It is proposed that the model presented in this paper could be incorporated into the software of a digital x-ray system. To do so, this would require measurements of varying µGy / mAs with kV_p and field size and appropriate calibration of the digital detector. Manufacturing tolerances are such that a single set of measurements on one system by the manufacturer could be applicable across all equivalent models of the x-ray system. The same is likely to be true of the digital detector; as

manufacturers have an intended calibration for their PV response, it is likely that calibrations undertaken on a single detector could be applicable across all equivalent models.

Whilst the work presented in this paper was undertaken on a Philips radiographic x-ray system and Fuji CR, it is believed it would work on any manufacturer's x-ray system provided there is a stable output and detector kerma – PV calibration. A single calibration is all that would be required on any system since the quality of the x-ray beam exiting the attenuator is independent of the detector.

The software programming represents the greatest barrier to this method being commercially adopted. The requirement would be for the system to produce an unprocessed version of the image and automatically take a PV measurement from an ROI within the image then use these numbers with the appropriate values from the look up tables to estimate the patient thickness.

The next step for this work is a test of the accuracy of the model on patients. Preparations are underway for a clinical trial to test the accuracy of the computational model under clinical conditions for abdominal examinations.

6   Conclusion

A computational model has been presented for estimating the thickness of a uniform attenuator using a single radiographic image and pre-measured data pertaining to the unique characteristics of the x-ray system and detector. The results are promising, with absolute deviations between estimated and known thicknesses of 0.5 – 10.8mm recorded. The estimates of thickness made using the model compare well against an approach involving manual calculation using data measured at the time of the exposure, for which the deviations between estimated and known thicknesses ranged between 0.02 – 11.6mm.

These deviations are of a magnitude that could be accepted for the intended clinical use of estimating paediatric patient thickness for the purposes of patient dose audit given the other options available.

References

[1] Hart D, Wall B F, Shrimpton P C, Bungay D R, Dance D R. *R318-Reference Doses and Patient Size in Paediatric Radiology*, NRPB 2000

[2] IAEA human health series. *Report 24 – Dosimetry in Diagnostic Radiology for Paediatric Patients*, IAEA 2013

[3] Hart D, Hillier M C, Wall B F. *W14 – Doses to patients from medical x-ray examinations in the UK – 2000 review*. NRPB 2002

[4] Hart D, Hillier M C, Wall B F. *29 – Doses to patients from radiographic and fluoroscopic x-ray imaging procedures in the UK – 2005 review.* HPA 2007

[5] Hart D, Hillier M C, Shrimpton P C. *34 – Doses to patients from radiographic and fluoroscopic x-ray imaging procedures in the UK – 2010 review.* HPA 2012

[6] IPEM DRL working party. *Guidance on the establishment and use of diagnostic reference levels for medical x-ray examinations.* IPEM report 88 (York: IPEM) 2004

[7] BEIR VII. Committee to Assess Health Risks from Exposure to Low Levels of Ionising Radiation. *Health risks from exposure to low levels of ionizing radiation BEIR VII Phase 2.* National research council of the national academies. The National Academies Press, Washington DC 2006

[8] Asai Y, Uemura M, Matsumoto M, Kanamori H. Dependence of radiographic sensitivity of CR imaging plate on X-ray tube voltage. Radiol Phys Technol 2008; 1:100-5.

[9] sunnuclear.com. Gammex, Inc. Middleton, WI. Solid Water HE & TMM product datasheet: 2015 [cited 21st June 2017].
Available from https://www.sunnuclear.com/documents/datasheets/SolidWaterHE-TMM_D070115.pdf

[10] Bohmann I. Ermittlung der Durchstrahlungsdurchmesser bei Säuglingen, Kindern und Jugendlichen zur Aufstellung von Belichtungswerten in der Röntgendiagnostik und Abschätzung der Organdosiswerte bei typischen Röntgenuntersuchungen. Munich, Gesellschaft für Strahlen und Umweltforschung, GSF 16/90 (1990)

[11] Lindskoug B A. Exposure parameters in x-ray diagnostics of children, infants and the newborn. Radiat Prot Dosim 1992; **43**(1/4): 289-92